

# Effect of Winter Snow and Ground-Icing on a Svalbard Reindeer Population: Results of a Simple Snowpack Model

Jack Kohler and

Ronny Aanes

Norwegian Polar Institute, N-9296 Tromsø,  
Norway.  
jack.kohler@npolar.no

## Abstract

Winter climate is a key factor affecting population dynamics in high-arctic ungulates, with many studies showing a strong negative correlation of winter precipitation to fluctuations in population growth rate. Terrestrial ice crust or ground-ice can also have a catastrophic impact on populations, although it is rarely quantified. We assess the impact of winter climate on the population dynamics of an isolated herd of Svalbard reindeer near Ny-Ålesund with a retrospective analysis of past winter snowpack. We model landscape-scale snowpack and ground-ice thickness using basic temperature and precipitation data in a simple degree-day model containing four adjustable parameters. Parameter values are found that lead to model snow and ground-ice thicknesses which correlate well with three different model targets: reindeer population growth rates; April snow accumulation measurements on two local glaciers; and a limited number of ground-icing observations. We explain a significant percentage (80%) of the variance in the observed reindeer population growth rate using just the modeled mean winter ground-ice thickness in a simple regression. Adding other explanatory parameters, such as modeled mean winter snowpack thickness or previous years' population size does not much improve the regression relation.

## Introduction

Population dynamical studies often show that observed fluctuations in large herbivore population size arise from both density dependence and environmental stochasticity (Sæther, 1997; Grenfell et al., 1998; Gaillard et al., 1998, 2000; Post and Stenseth 1999; Coulson et al., 2001). In both temperate and arctic areas, winter climate has often been found to influence large herbivore population dynamics, commonly with a negative relationship between amount of snow and population parameters such as growth rate, survival or fecundity (Fancy and White, 1985; Adamczewski et al., 1988; Sæther, 1997; Gaillard et al., 1998; Post and Stenseth, 1999; Post and Forchhammer, 2003).

This pattern also includes Svalbard reindeer (*Rangifer tarandus platyrhynchus*) where both density dependence and a strong negative relationship between population growth rate and winter precipitation amount have been identified (Aanes et al., 2000, 2003; Solberg et al., 2001). Snow both reduces access to available food and increases energetic costs. This may reduce female fecundity and increase the mortality, especially for the youngest individuals (see Sæther, 1997; Gaillard et al., 1998 for reviews).

A less-studied climatic phenomenon is the formation of terrestrial ice-crust or ground-ice. It has long been appreciated that ground-icing events have a strong impact on population dynamics since they can completely block access to the food eaten by large herbivores. Formation of ground-ice, leading to a decrease in population size, or even to population crashes, has been reported both on Svalbard (Lønø, 1959; Alendal and Byrkjedal, 1974; Larsen, 1976; Reimers, 1977, 1982, 1983; Tyler, 1987; Øritsland, 1998), as well as in other areas (e.g., Parker et al., 1975; Forchhammer and Boertmann, 1993). Few of these studies have actually tried to systematically quantify the impact of icing on the dynamics; most studies report single observations of population decreases after severe winters. One exception is from Greenland, where Forchhammer and Boertman (1993) calculated an index to reflect the formation of ground-ice and evaluated how it affected muskox populations. Another example comes from Svalbard where Solberg

et al. (2001) found a negative relationship between number of winter warm days ( $>0^{\circ}\text{C}$ ) with precipitation and Svalbard reindeer population growth rate. Finally, Putkonen and Roe (2003) look explicitly at the effect of rain-on-snow events, the main contributing factor leading to ground-icing. However, while they discuss qualitatively the effect this may have on biota, they did not include any of the available ecological data, on the local reindeer population, for example.

In the present paper we use information from a well-studied Svalbard reindeer population on the Brøgger peninsula area, near Ny-Ålesund (Fig. 1). A previous study found no evidence of strong density dependence operating in this population (Aanes et al., 2000). The strongest correlation was between the population growth rate ( $G$ ) (by custom referred to as  $R_t$  in the biological literature), given by

$$G(t) = \ln[N(t)] - \ln[N(t-1)], \quad (1)$$

a measure of the change in population size  $N$  between years  $t$  and  $t-1$ , and the summed winter (Oct.–Apr.) precipitation (Aanes et al., 2000). A dramatic effect of winter precipitation on this reindeer population is best exemplified by the ground-icing event that occurred on the Brøgger peninsula in autumn 1993. During an 8-d period in November and December, record amounts of rain fell, while air temperatures fluctuated around  $0^{\circ}\text{C}$ . Prior to the rainfall, there had been a prolonged cold period, with no snow, and ground temperatures were well below freezing. The net result was a thick ice layer (up to 10–30 cm) deposited over large parts of the lowland plain, and a substantial reduction in the reindeer population the following spring. While the population reduction was not wholly due to mortality (there was migration over the glaciers and frozen bays to previously uncolonized areas), a substantial number of reindeer died in the winter of 1993/94 due to the icing.

Given the apparent effect of winter precipitation on population change, we would expect that the relation between population growth rate  $G$  and winter precipitation is improved when one uses actual snowpack thickness data. Furthermore, there may have been other, less dramatic episodes of icing in the past, which were not noticed or deemed noteworthy, but which nonetheless restricted reindeer's access to food.

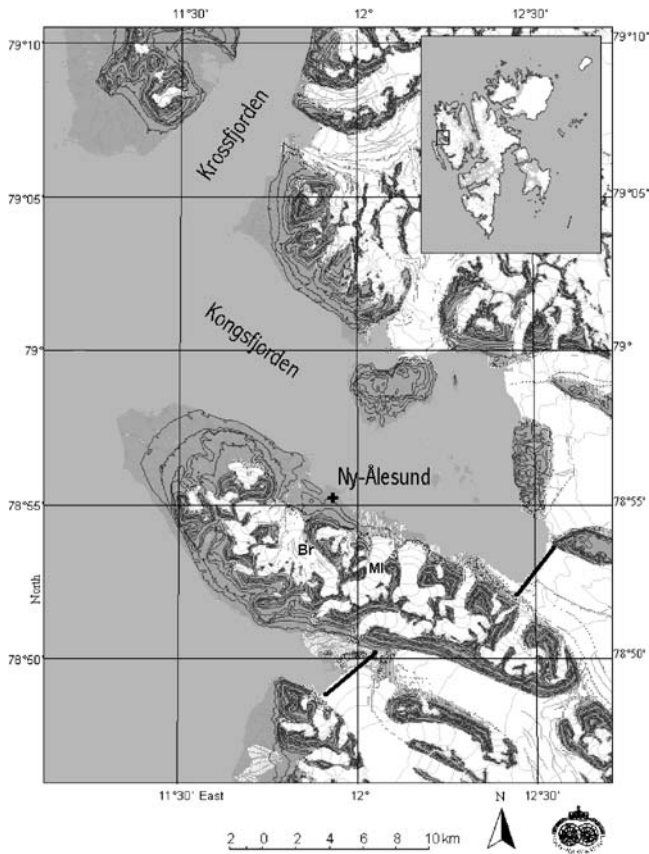


FIGURE 1. Brøgger peninsula, showing Ny-Ålesund, Austre Brøggerbreen (Br) Midre Lovénbreen (Ml), and natural barriers that impede migration from the peninsula (black lines). Inset shows location within Svalbard.

Even the most significant icing event, which is only reported orally (Aanes et al., 2002), was not measured systematically in the field, and until recently, there have been no regular observations of the snowpack in the area. Our only recourse, then, is to model the snowpack with available meteorological measurements. Using a simple snowpack model driven by twice-daily precipitation and temperature measurements, we retrodict snowpack thickness and the formation of ground-ice, and evaluate its importance for Svalbard reindeer dynamics in the area.

## Field Site and Data

### FIELD SITE

The Brøgger peninsula, located on the northwestern coast of Svalbard, is a rugged, glaciated mountain ridge, surrounded by an extensive lowland plain (Fig. 1). Total area is about 220 km<sup>2</sup>, of which 25% is glaciated and 50% contains 5% or greater vegetation coverage. Vegetation comprises small vascular plants, grasses, and cryptogams (Øritsland et al., 1980; Brattbakk, 1986). The climate is characterized by low mean annual temperature (−6°C), frequent winter warm temperature excursions, and low mean annual precipitation (400 mm).

### REINDEER

There were no Svalbard reindeer on the peninsula from the beginning of the 1900s, when the population was eradicated by hunting, until 1978, when 15 reindeer were introduced as part of a long-term ecology experiment. Open water and glacier fronts provide

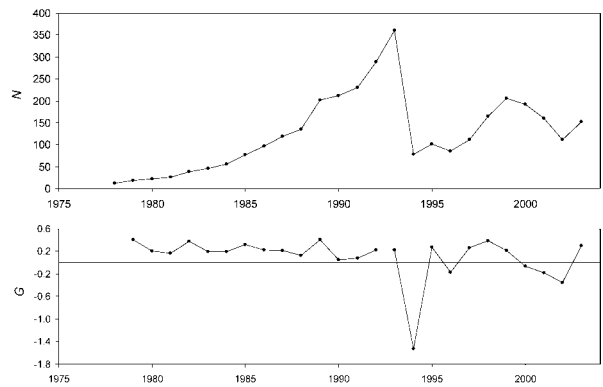


FIGURE 2. Population size  $N$  and log population growth rate  $G$  of Svalbard reindeer population on Brøgger peninsula, 1978–2002.

natural barriers to impede migration of the introduced population, under normal conditions (Fig. 1). From 1979 to the present, the total number of reindeer on Brøgger peninsula has been counted each spring (Aanes et al., 2000); these measurements are the basis for the annual population used in this paper (Fig. 2).

### METEOROLOGICAL MEASUREMENTS

Meteorological data from Ny-Ålesund for the period 1 January 1969–31 December 2002 are taken from routine measurements made by the Norwegian Meteorological Institute. Input data are twice-daily (0700 and 1900) measurements of standard 2-m screen air temperature and summed 12-h precipitation from a heated rain gauge. The twice-daily temperatures are averaged to estimate the effective temperature ( $T$ ) of the preceding 12-h period during which time an amount of precipitation ( $P$ ) collected in the rain gauge.

Precipitation data are not adjusted to account for wind speed, which reduces the amount of precipitation caught by the gauge, particularly for snow (Førland and Hanssen-Bauer, 2000), nor do we apply any elevational correction factor (Førland et al., 1997), since we have found that the model results are insensitive to either precipitation correction factors.

### SNOW AND ICE MEASUREMENTS

Very little is recorded about ground-icing, either on Svalbard in general or in Ny-Ålesund in particular. A summary of all known or measured icings on the Brøgger peninsula is given in Table 1. There are only sporadic measurements made of snow depth at the meteorological site in Ny-Ålesund proper. Long-term annual snow-depth measurements are available in the area from the winter glacier mass-balance records (e.g., LeFauconnier et al., 1999) of the nearby glaciers Midre Lovénbreen and Austre Brøggerbreen (Fig. 1). The mass-balance data used here (J. Kohler, unpublished data) cover the period 1970–2002, and comprise averages of snow-thickness measurements made in late April–early May at the lowest elevations (50–150 m). While restricted spatially to the two glaciers, the data (Fig. 3) are good proxies for spring snowfall over the entire Brøgger peninsula, as demonstrated by parallel measurements made over the period 2000–2003.

## Model

### MODEL DESCRIPTION

We use a simple degree-day model (e.g., Rango and Martinec, 1995) to simulate Ny-Ålesund snowpack and icing back in time. The

TABLE 1

All recorded observations of ground-ice formation in Ny-Ålesund, and values assumed for use in R3

Winter	Observed ground-ice thickness	Assumed for R3	Avg. best-guess model results
1993–1994	10–30 cm over wide areas	15 cm	18.5 cm
1995–1996	ca. 5–10 cm, where exposed	8 cm	10.9 cm
1999–2000	May, mean 37 pits: 2.9 cm	3 cm	2.5 cm
2001–2002	May, mean 36 pits: 6.1 cm	6 cm	5.7 cm

model is essentially a nonlinear filter operating on time-series of temperature ( $T$ ) and precipitation ( $P$ ). The filter highlights the thresholds and interactions between  $T$  and  $P$  that provide the fundamental controls on whether or not ground-icings can form. Our model is not a “physical” snowpack model, such as SNTHERM (Jordan, 1991) or SNOWPACK (Bartelt and Lehning, 2002), which can simulate the detailed layer structure within a time-varying snowpack. Physical models are inappropriate for the problem at hand for several reasons. First, they include a large number of relevant but difficult to model processes (e.g., snowpack densification, snow crystal metamorphosis, and water transport) which require *in situ* measurements to parameterize or verify. Second, the input and verification data are difficult to obtain as continuous time-series since they generally require precise calibration and a high degree of homogenization (e.g., radiation, albedo, wind profiles). Third, and more importantly, the results from physical models still need to be extrapolated to the larger landscape or regional scale from the location(s) in which the required data are available. Since in most cases the extrapolation is as poorly constrained for physical models as it is for simpler models, it ultimately comprises the largest source of mismatch between model and reality (Rango and Martinec, 1995).

The model (Fig. 4) comprises two boxes: a snowpack box and a ground-ice box. Precipitation occurs either as rain or as snow; snow is added to the snowpack box, while rain or water formed from melting in the snowpack box is assumed to pass directly into the ground-ice box. Melting of snow or ground-ice follows the degree-day concept, that is, the amount of melt is indexed to the number of degrees per day above a certain threshold (Rango and Martinec, 1995).

Four parameters control the behavior of the model: two threshold temperatures,  $T_{SR}$  and  $T_{DD0}$ , the first of which determines the precipitation type and the second of which determines the temperature above which snow can melt, and two degree-day coefficients,  $DD_S$  and  $DD_I$ , which control the amount of snow and ice melt.

Input data are air temperature  $T(t)$  and precipitation  $P(t)$  as a function of time  $t$ . At each time-step  $t_i$ , when the air temperature  $T(t_i)$  is less than a threshold temperature  $T_{SR}$ , precipitation occurs as snow, and the snowpack thickness  $S(t_i)$  increases by the precipitation amount  $P(t_i)$ . When  $T(t_i)$  is greater than or equal to  $T_{SR}$ , precipitation occurs as rain. Rain is assumed to pass through the snowpack box to fill the ground-ice box by the precipitation amount  $P(t_i)$ , if the ground is frozen (we assume this to be the case between the months of October and May; see below for further discussion).

When  $T(t_i)$  is greater than a second threshold temperature  $T_{DD0}$ , the snowpack thickness  $S(t_i)$  is reduced at a rate  $DD_S [T(t_i) - T_{DD0}]$ . Melted snow is treated like rain, as described above, moving to the ground-ice box when the ground is frozen. If the snowpack is absent then the ground-ice melts at a second rate  $DD_I [T(t_i) - T_{DD0}]$ .

Melting ice, or any melt or rain falling between June and September, passes out of the model. Snow or ice remaining in the model at 1 August is removed.

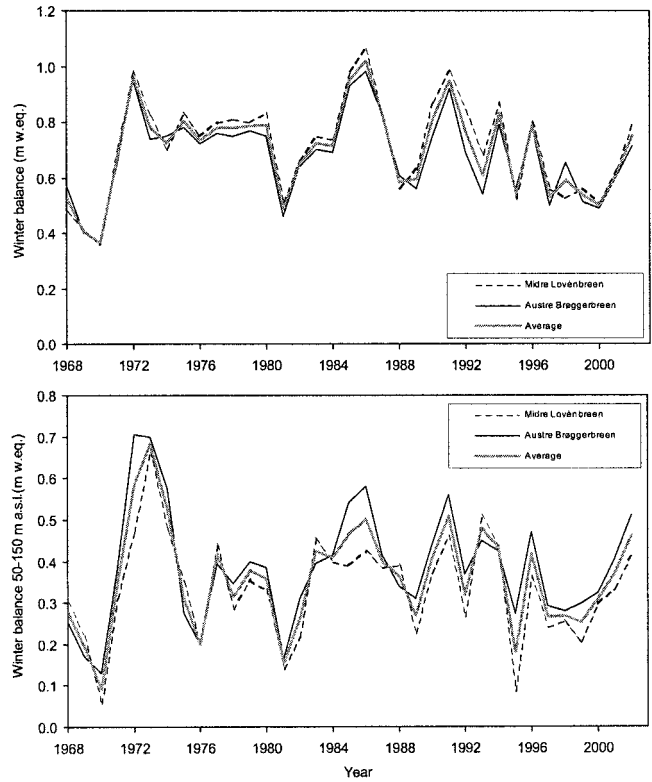


FIGURE 3. Winter mass balance for Midre Lovénbreen and Austre Brøggerbreen (1968–2002) averaged over the entire glacier (upper figure) and for the lowermost elevation intervals 50–150 m a.s.l. (lower figure).

MODEL ASSUMPTIONS

Snowpack density is not considered in the model; water formed in the snowpack simply passes directly to the bottom to form ground-ice, neglecting the possibility that ice or high density layers form within the snowpack. For the problem at hand, modeling the effect of winter snowpacks on reindeer, this is not a completely unreasonable simplification since the formation of ice layers anywhere within the

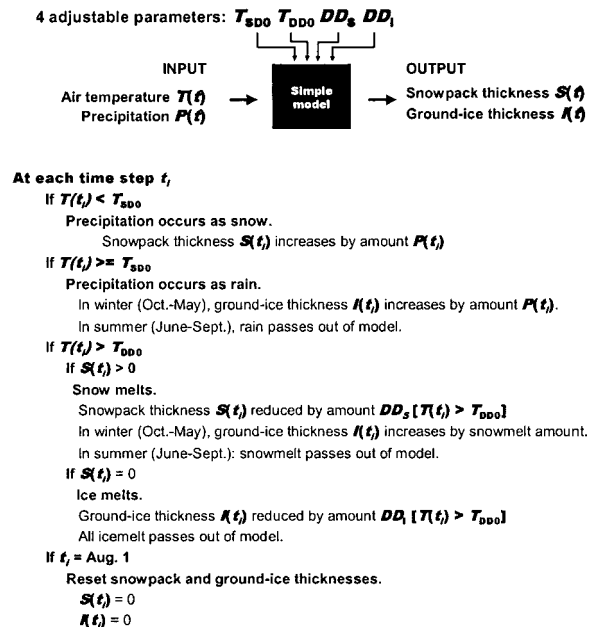


FIGURE 4. Snowpack model schematic.

TABLE 2

Range and step-size (see text) of parameter values used in modeling

	$T_{SR}$ (°C)	$T_{DD0}$ (°C)	$DD_S$ (mm °C <sup>-1</sup> )	$DD_I$ (mm °C <sup>-1</sup> )
Min	-1	-3	4	4
Max	5	5	16	16
Step-size	1	1	2	2

snowpack provides a similar, albeit more easily breached, physical barrier to the food source.

We ignore the complication of modeling the heat budget of the ground and the snow layer (e.g., Putkonen and Roe, 2003), since this introduces new assumptions and parameters concerning land-surface, soil, and permafrost properties. Instead we simply assume that the ground is frozen between the months of October and May. Records of ground temperature from the Ny-Ålesund area show that this assumption is not unreasonable (Putkonen, 1998; Roth and Boike, 2001; Boike et al., 2003; S. Gerland, unpublished data), although Putkonen and Roe (2003) show that the latent heat released in freezing during one major mid-winter icing event on the Brøgger peninsula raised the ground temperature to the freezing point. Nevertheless, this effect is short term and furthermore may not reflect the temperature at the icing surface.

Finally, we remove all remaining snow and ice on 1 August, if necessary. This is functionally equivalent to allowing higher summer ice melt rates, or in other words, temporally varying  $DD_I$ . Degree-day factors do in fact vary seasonally (e.g., Rango and Martinec, 1995), but accounting for this in the model adds to model complexity. In any case, our application of the model in this paper is directed to winter effects. At this point we have too few data to constrain the behavior of the model in summer, apart from our observations of an ice-free landscape in all summers we have been there.

#### PARAMETER CHOICE

Landscape-scale models that use the degree-day approach (e.g., Rango and Martinec, 1995; Lindström et al., 1997) typically need to be calibrated, that is, model parameters must be adjusted to get the best fit of observed to modeled data. Parameter values reported in the literature, particularly degree-day coefficients, can vary widely (e.g., Braithwaite, 1995; Rango and Martinec, 1995; Hock, 1999, 2003; LeFebvre et al., 2002). Therefore, we cannot simply assume that the parameters take on any reported values.

We explore parameter space to see how different values affect the model results. We assess model goodness-of-fit using the following targets: (1) the reindeer log population growth rate  $G$  (Fig. 1), which we assume to be a ground-icing proxy (2) the winter mass-balance measurements (Fig. 3), and (3) the few observations of icing (Table 1).

It may seem imprudent to use reindeer population growth rate as a ground-icing model target, without considering any other internal population factors, but given that previous work has demonstrated a clear connection between winter precipitation and population change (Aanes et al., 2000, 2003), and that two of the major population downturns occurred in years for which we do know there was icing (Table 1), it is not entirely unwarranted to use changes in the reindeer population as a ground-icing indicator. Furthermore, there are simply too few measurements of ground-icings (Table 1) to use these data exclusively as a model target. Finally, it is not possible to use the mass-balance data as a ground-icing model target since these data are snow depths, that is, the thickness obtained from probing the snowpack until something hard is reached. Whether this is ground or ground-ice is not recorded, so that in this case the comparison of modeled to observed data would be completely insensitive to the choice of parameters that suppress or promote model ground-icing.

#### MODEL CALIBRATION

The output data from the model are time-series of twice-daily snowpack thickness  $S$ , and ground-ice thickness  $I$ . We assume an expected range of values for the model's four adjustable parameters and, moving systematically at reasonable step-sizes between these minimum and maximum values (Table 2), obtain trial  $S^*$  and  $I^*$  time-series for each combination of parameters. The trial model results are then compared quantitatively to targets via three regressions.

#### REGRESSION 1

The first (hereafter referred to as R1) is a multiple linear regression that assumes that reindeer log population growth can be modeled simply by

$$\hat{G} = c_1 + c_2 S_w^* + c_3 I_w^{*2}, \quad (2)$$

Here  $S_w^*$  is the average winter (Oct.–Apr.) snowpack thickness,  $I_w^*$  is the average winter (Oct.–Apr.) ground-ice thickness, and both quantities are derived from model  $S^*$  and  $I^*$  trial time-series for the years 1979–2002. Hatted variables denote a regression result. The coefficients  $c_i$  in equation (2) are determined from the regression, whose goodness-of-fit is evaluated by the familiar regression coefficient  $r^2$  (Davis, 2002).

Thus for each combination of the four adjustable model parameters, we obtain a value of  $r^2$  which indicates how well the  $S_w^*$  and  $I_w^*$  values obtained with those parameters did at explaining the observed reindeer population growth rate for the years 1979–2002.

Squaring the  $\bar{I}_w$  term in equation (2) is a simple, low parameter cost way of expressing the nonlinear threshold effect of ground-ice on reindeer population dynamics. Ground-ice should have a threshold effect because thin ice layers provide little resistance to the sharp hooves of Svalbard reindeer. Above a certain thickness, however, there is an increasing energy cost to break through. Furthermore, the thicker the ground-ice layer is at an arbitrary point, the greater is the portion of the landscape covered by ground-ice.

#### REGRESSION 2

The second regression (R2) compares model 1 May snowpack thickness  $S_{M1}^*$  to  $b_{w100}$ , the winter mass-balance data for the period 1970–2002 (Fig. 3) via

$$\hat{b}_{w100} = c_4 S_{M1}^*, \quad (3)$$

where  $c_4$  is a coefficient determined in the regression. In R2 we force the regression to pass through the origin. We also assume that winter mass balance was measured each year on 1 May. The actual dates vary by as much as 2 wk around this date, but are essentially unknown for much of the measurement period. This would contribute only small differences between model and observed data, however, since snowpack thickness is highly correlated over such short timescales during this period.

#### REGRESSION 3

The third regression (R3) compares  $I_M$ , the four observations of icing thickness (Table 1), to the simulated May 1 ground-ice thickness  $I_{M1}^*$  via

$$\hat{I}_{M1} = c_5 I_{M1}^*, \quad (4)$$

where  $c_5$  is a coefficient determined in the regression. Data from 1995/96 is a qualitative observation, so we assume a value for that year (Table 1).

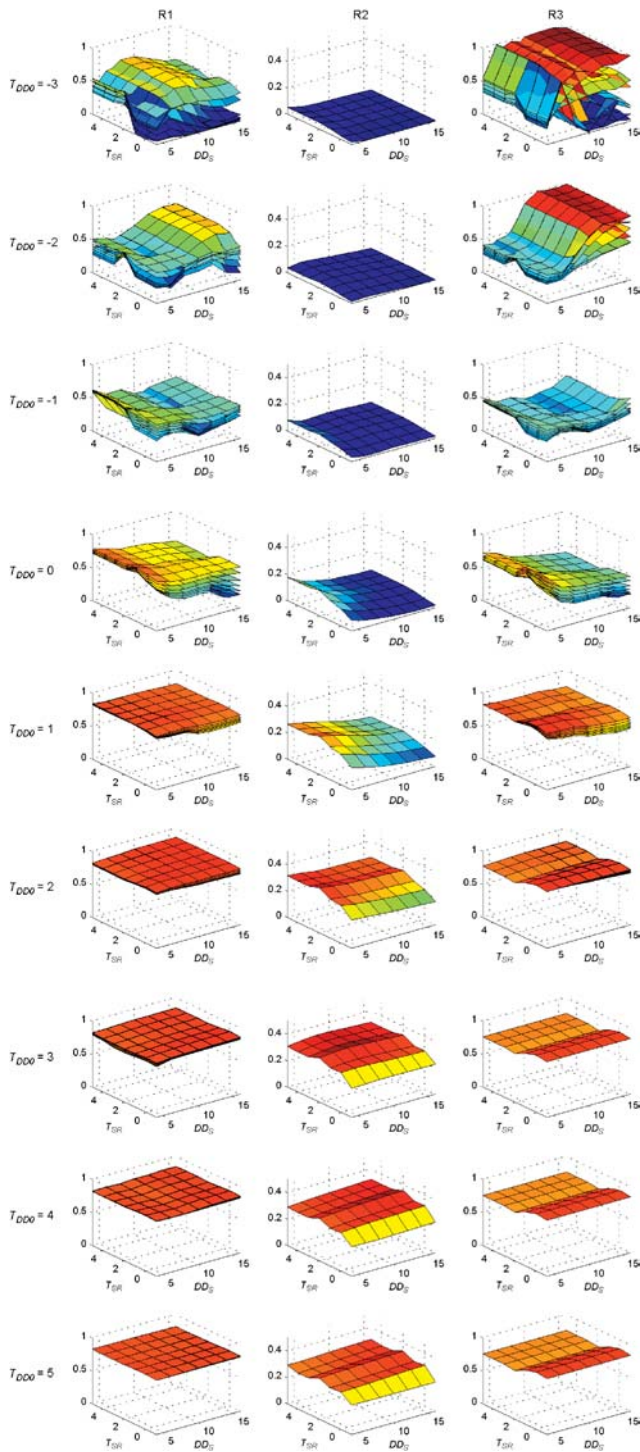


FIGURE 5. Regression coefficient  $r^2$  surfaces as a function of  $T_{SR}$  and  $DD_S$ , organized in rows by different values of  $T_{DDO}$ , and in columns by results of R1, R2, and R3. Multiple surfaces in plot correspond to different values of  $DD_I$ .

### Regression Results

For each regression R1-R3, goodness-of-fit coefficients ( $r^2$ ) are computed for every combination of the four model parameters  $T_{DDO}$ ,  $T_{SR}$ ,  $DD_S$ ,  $DD_I$ . Figure 5 shows plots of the  $r^2$  surfaces as a function of  $T_{SR}$  and  $DD_S$ , organized by regression number (R1-R3) and different values of  $T_{DDO}$ ; multiple surfaces within one plot correspond to different values for  $DD_I$ . Figure 6 shows histograms of values for the occurrence of the

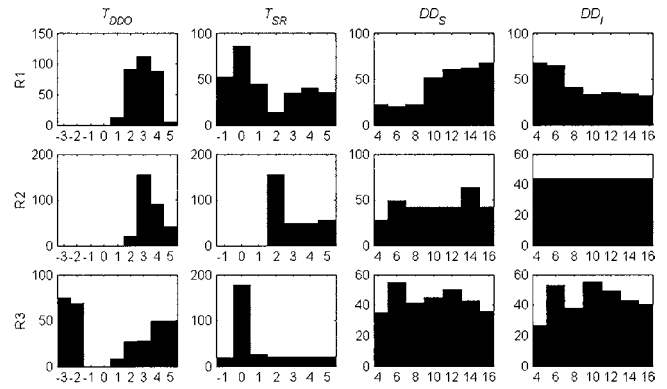


FIGURE 6. Histograms of four model parameters  $T_{DDO}$ ,  $T_{SR}$ ,  $DD_S$ , and  $DD_I$  (columns) obtained from the 95th percentile or better results of R1-R3 (rows).

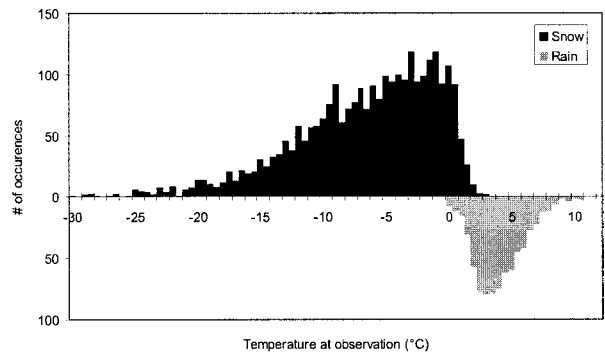


FIGURE 7. Histogram of number of rain or snow occurrences as a function of reported temperature at observation time, based on available data from Ny-Ålesund 1969–2002.

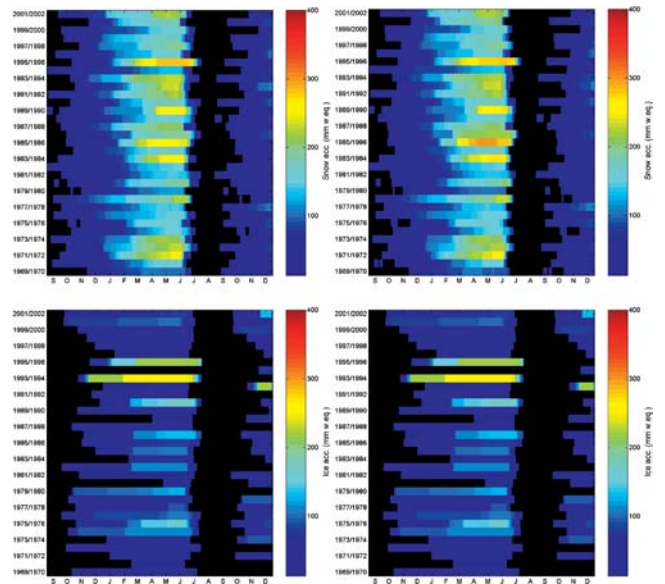


FIGURE 8. Raster plot of simulated winter snowpack (upper plots) and ground-ice thicknesses lower plots). Plots on left are for best-guess  $S^{BG}$  and  $I^{BG}$  (left panels) and on the right for the average of the 300 best simulations.

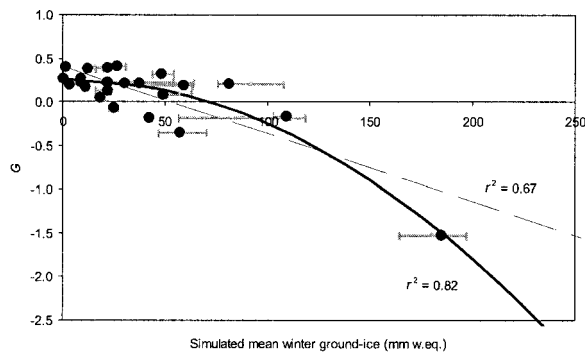


FIGURE 9. Winter mean ground-ice thickness  $\bar{I}_w^{BG}$  compared to  $G$  (black points). Thick and dashed lines are parabolic and linear fits of  $\bar{I}_w^{BG}$  to  $G$ . Gray points and lines show means and 1 S.D. of winter mean ground-ice thicknesses obtained from 300 best simulations.

four model parameters for >95th percentile results in each individual regression R1-R3, about 300 model results for each regression.

#### BEST VALUES FOR $DD_S$ AND $DD_I$

In the R1 and R3 plots (Fig. 5), surfaces with lower regression coefficients generally correspond to higher values of  $DD_I$ . In the R2 plots there is only one surface since the simulations lead to identical results regardless of the choice of  $DD_I$ , not surprising given that R2 is based only on observed snowpack thickness. There is little difference, however, in R1 and R3 for different values of  $DD_I$  at  $T_{DDO} \geq 2$ , the area of parameter space in which all three regressions have maximum  $r^2$ .

The best regression results for  $DD_S$  (Fig. 6) tend to lie toward values ( $\geq 10$  mm  $^{\circ}\text{C}^{-1}$ ) higher than those reported in Hock (2003) for a variety of mountainous settings, although Lefebvre et al. (2002) find values as high as 14 mm  $^{\circ}\text{C}^{-1}$ .

In contrast, the best fits in R1 are associated with lower values of  $DD_I$  (Fig. 6). Values of  $DD_I$  are typically about 50% greater than  $DD_S$  (e.g., Hock, 2003); however, although lower values of  $DD_I$  appear to be preferred by R1, higher values lead to nearly equally good fits, as judged from the relatively close-spaced surfaces for  $T_{DDO} > 1$  (Fig. 5). Furthermore, the flatness of surfaces in areas with the highest  $r^2$  values (Fig. 5) shows that there are no truly preferred values for  $DD_S$ .

#### BEST VALUES FOR $T_{DDO}$

R1 and R2 both show the highest values for  $T_{DDO} > 0^{\circ}\text{C}$ . R3 has two maxima, one at low values of  $T_{DDO}$  ( $-3$  to  $-2^{\circ}\text{C}$ ) and the other at higher values (Fig. 5). Low values of  $T_{DDO}$  result in more modeled ground-ice due to an increased incidence of melted snow; however, this does not necessarily reflect reality given that R3 is based on only four points, two of which are poorly constrained. Furthermore, the high  $r^2$  values at low values of  $T_{DDO}$  are associated with unrealistically low values of  $DD_I$ . Increasing  $DD_I$  leads to a substantial reduction in the goodness of fit.

Accordingly, we assume that despite the first maximum in R3, all of the regression results consistently indicate only positive value for  $T_{DDO}$ . For R1 and R2, best fits are obtained with  $T_{DDO}$  at around  $3^{\circ}\text{C}$ , while in R3, best fits occur at 2 to  $5^{\circ}\text{C}$  (Fig. 6). In the literature (e.g., Rango and Martinec, 1995)  $T_{DDO}$  is generally taken to be  $0^{\circ}\text{C}$ , so that starting melt only for temperatures higher than  $3^{\circ}\text{C}$  or more may seem unduly high. Part of the positive offset (ca.  $0.5^{\circ}\text{C}$ ) could be explained by the temperature lapse-rate, since the model driving data are taken at near sea level while the observed data used in the regressions are effectively from higher elevations. Another possibility is that while snowmelt does in fact occur when temperatures are around  $0^{\circ}\text{C}$ , this water typically

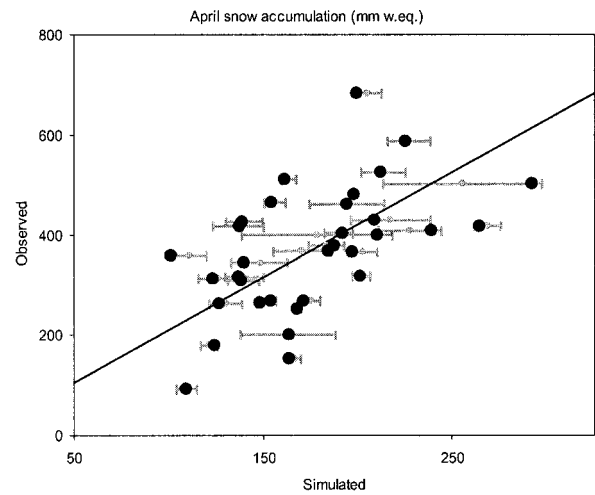


FIGURE 10. May 1 snowpack thickness  $S_{M1}^{BG}$  compared to observed mass balance (black points). Line shows linear fit passing through the origin. Gray points and lines show means and 1 S.D. of May 1 snowpack thicknesses from 300 best simulations.

refreezes in the snowpack. Snowmelt only goes to bottom of snowpack to form ground-icing when higher temperatures are reached. A final possibility concerns seasonality in degree-day factors (Rango and Martinec, 1995). The combination of relatively high values of  $T_{DDO}$  and constant degree-day factors serves to reduce winter melting and increase summer melting, duplicating the usual pattern for temporally-varying  $DD_S$  and  $DD_I$  (Rango and Martinec, 1995).

#### BEST VALUES FOR $T_{SR}$

In R1 the effect of  $T_{SR}$  is fairly weak (Fig. 5), although there is a slight preference for  $T_{SR} = 0^{\circ}\text{C}$  (Fig. 6), while in R3, there is a clear maximum for  $T_{SR} = 0^{\circ}\text{C}$  (Figs. 4, 5). The best fits in R2, on the other hand, occur predominantly at  $T_{SR} = 2^{\circ}\text{C}$  (Fig. 6). In either case, however, the obtained values are close to that indicated by the relation between observed precipitation type and 2-m temperature, whose transition occurs over the range  $0$ – $2^{\circ}\text{C}$  (Fig. 7) as judged from the available data at Ny-Ålesund of observed precipitation type grouped by temperature at the observation time. The difference probably relates to the quantities being regressed; R1-R3 primarily respond to modeled ground-ice, which give better results with more rain (lower  $T_{SR}$ ), while R2 gives best results when there is more snow (higher  $T_{SR}$ ).

### Best-Guess Model Snowpack

To summarize, model calibration shows that the good fits in R1-R3 occur over a wide range of parameter values, and that, with the possible exception of  $T_{DDO}$ , these values are at least in the vicinity of expected or previously reported values. Accordingly, we now model a time-series of the “best-guess” snowpack thickness  $S^{BG}$  and ground-icing thickness  $I^{BG}$  (Fig. 8) using parameter values ( $T_{DDO} = 3^{\circ}\text{C}$ ,  $T_{SR} = 1^{\circ}\text{C}$ ,  $DD_S = 8$  mm  $^{\circ}\text{C}^{-1}$ ,  $DD_I = 12$  mm  $^{\circ}\text{C}^{-1}$ ) which could be taken from the literature, but which are guided to some extent by the results of R1-R3. The model is relatively insensitive to the ultimate choice of adjustable parameters, however, as demonstrated by comparing  $S^{BG}$  and  $I^{BG}$  to average thicknesses obtained from the 300 best simulations, the latter having been obtained by ranking the sum of the normalized  $r^2$  score in R1-R3. Qualitatively, there appears to be little difference between the two simulations (Fig. 8). Comparing observed  $G$  to the mean winter (Oct.–Apr.) ground-ice thickness  $\bar{I}_w^{BG}$ , as well as those obtained from the 300 best simulations, shows that the two have consistent values for

TABLE 3

Results of regressions of observed  $G$  against various parameters (see text) for the period 1978/79 to 2001/02. All regressions include a constant term. Table (a) uses all data, (b) removes data from 1993/94, and (c) also removes data from 1995/96. Each regression is numbered and includes one or more parameters (indicated by crosses). Bold indicates regression results significant at  $P = 0.05$  or better.

	$\sum P_w$	$S_{M1}^{BG}$	$[\bar{I}_w^{BG}]^2$	$\ln N(t-1)$	$r^2$	DF	F	P
<b>a</b>								
1	X				<b>0.44</b>	22	17.5	<0.001
2		X			0.12	22	3.1	0.096
3			X		<b>0.82</b>	22	97.8	<0.001
4				X	<b>0.22</b>	22	6.3	<b>0.019</b>
5	X	X			<b>0.84</b>	21	54.0	<0.001
6	X	X	X		<b>0.88</b>	20	49.1	<0.001
<b>b</b>								
1	X				<b>0.29</b>	21	8.5	<b>0.008</b>
2		X			0.06	21	1.3	0.284
3			X		<b>0.31</b>	21	9.2	<b>0.006</b>
4				X	<b>0.18</b>	21	4.5	<b>0.043</b>
5	X	X			<b>0.37</b>	20	5.9	<b>0.011</b>
6	X	X	X		<b>0.53</b>	19	7.0	<b>0.002</b>
<b>c</b>								
1	X				0.18	20	4.2	0.053
2		X			0.02	20	0.4	0.534
3			X		<b>0.19</b>	20	4.8	<b>0.040</b>
4				X	<b>0.19</b>	20	4.7	<b>0.040</b>
5	X	X			<b>0.29</b>	19	3.8	<b>0.043</b>
6	X	X	X		<b>0.46</b>	18	5.2	<b>0.009</b>

most years (Fig. 9). This is likewise the case for a comparison of observed mass balance to the mean 1 May snowpack thickness  $S_{M1}^{BG}$  computed from the best-guess and the 300 best simulations (Fig. 10).

Figure 10 also shows that modeled snowpack thicknesses are roughly half of those actually observed. This may be due to a number of factors, including spatial variability, elevation difference (Førland et al. [1997] report a ca. 20–25% increase in precipitation per 100 m elevation), and wind (which not only reduces precipitation catch in the gauge but are often stronger in Ny-Ålesund than on the glaciers).

### Snow, Ice, and Reindeer Dynamics

We now apply two annual ground-ice and snow parameters  $[\bar{I}_w^{BG}]^2$  and  $S_{M1}^{BG}$  derived above. We regress the observed reindeer population growth rate  $G$  against different combinations of these two modeled parameters as well as two observed parameters, summed winter (Oct.–Mar.) precipitation  $\sum P_w$ , and log of the previous years' population  $\ln N(t-1)$ . All regressions include a constant term. The parameters used in each regression and the resultant statistics are given in Table 3. Note that we do not combine regressions involving  $\sum P_w$  and the modeled parameters since they are strongly correlated. Regressions are performed for all data from 1978/79 to 2001/02 (Table 3a), for all data but removing the extreme ground-icing year 1993/94 (Table 3b), and for all data but removing both 1993/94 and 1995/96 (Table 3c). The latter regressions are to test the robustness of the results when removing the extreme events.

As expected, there is a negative relationship between  $G$  and all winter climate parameters. And as reported previously (Aanes et al., 2000), the regression of  $G$  and  $\sum P_w$  explains a significant amount of variance. But when considering all of the data, the square of the ground-icing parameter  $[\bar{I}_w^{BG}]^2$  alone (regression 3, Table 3a) is by far the best single parameter for explain fluctuations in reindeer population

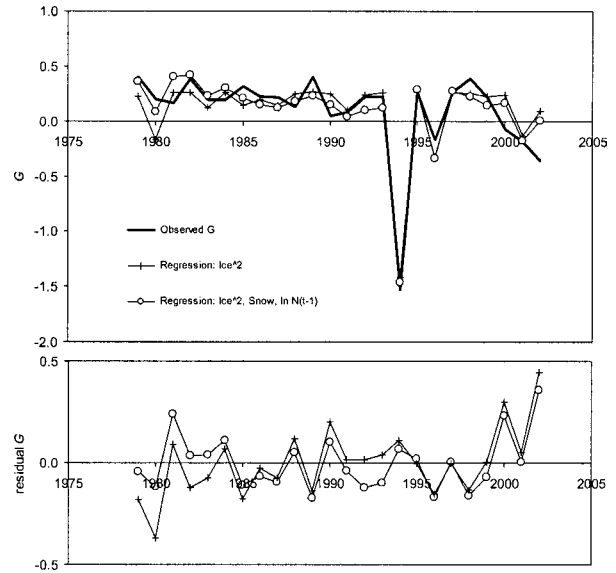


FIGURE 11.  $G$  observed (black line) and calculated using two regressions (3 and 6 in Table 3a). One regression (crosses) uses just  $[\bar{I}_w^{BG}]^2$  and the second (circles) includes  $S_{M1}^{BG}$  and the previous year's population  $N(t-1)$ . The lower panel shows the regression residuals.

growth rate, explaining more than twice the variance as explained by  $\sum P_w$  alone (regression 1, Table 3a). Adding additional parameters in the regressions (e.g., regressions 5 and 6, Table 3a) does not improve greatly the amount of variance explained.

A time-plot of  $G$  obtained from regression of the ground-icing parameter shows that it captures the dynamics reasonably well (Fig. 11). There is, however, a temporal trend to the residuals ( $r^2 = 0.28$ ), with an increasing tendency toward over-prediction of the population growth rate with time. Although this temporal trend is dependent entirely on the first two and last three points, a likely explanation could lie in the grazing history of Brøgger peninsula. The reindeer were introduced to an area with superabundant resources, since there had been no grazing for roughly 100 yr. After the increase and crash in the reindeer population, studies have shown that the vegetation has been both reduced in amount and altered in composition (e.g., Cooper and Wookey, 2001; Henriksen et al., 2003). Hence, there has been an increasing imbalance between available food and reindeer density, and extreme climatic events such as ground-icings could be having an increasingly deleterious effect on the reindeer population.

Including the snowpack parameter  $S_{M1}^{BG}$  (regression 5, Table 3a) does not alter the basic result obtained using the ground-ice parameter alone; there is a slight improvement in the goodness-of-fit, but the temporal trend in the residuals (not shown) remains. However, while including the previous year reindeer density does not increase the goodness-of-fit by much (regression 5, Table 3a), it does reduce the temporal trend in the residuals (Fig. 11). While the temporal trend is highly dependent on a few data-points at the beginning and end of the time-series, we would argue nonetheless that the existence of a trend shows that the importance of population density has increased with time. This is to be expected in introduced populations following their initial growth phase with abundant food supply. Strong density dependence likely resulting from food competition has been found in two other Svalbard reindeer populations (Aanes et al., 2003), and we expect the Brøgger population to more or less mirror this dynamical pattern in the future, that is, with density dependence and environmental stochasticity operating in concert to influence the population dynamics.

There are three final points to consider. The first is that since

ground-icing and  $G$  appear to resemble one another mostly on the basis of just two data points, it is natural to suspect that these extreme events alone are responsible for the high values of  $r^2$ . Removing one or both years with heavy icing from the regressions (Table 3b, 3c) does result in a drop in the amount of variance explained by the ground-icing parameter. In fact, for the case in which we remove both extreme years, any of the parameters used alone (except snowpack) explain a similar amount of variance in  $G$ . Now the full regression (regression 6, Table 3c) explains more variance than the ground-icing parameter alone, implying that there is some underlying density-dependence in the population dynamics (see above). In addition, while  $r^2$  values decline in all regressions when removing the extreme years, the regression constants (not shown) obtained do not vary by much, suggesting that the regressions relations between the various parameters and  $G$  are relatively robust and not overly guided by outlier values.

The second point is that the ground-icing parameter  $[\bar{I}_w^{BG}]^2$  was developed, in part, using precisely a regression involving the reindeer population (regression 5, Table 3a is identical to equation 2), so it may seem like circular reasoning to commend the snowpack model on its performance in predicting reindeer population growth. We have demonstrated, however, that the snowpack model results are insensitive to choice of model adjustable parameters. Furthermore we obtain similar results selecting the adjustable model parameters based on the R2 and R3 results alone.

Finally, as mentioned previously, squaring the ground-ice term  $\bar{I}_w^{BG}$  is a simple, low parameter cost way of expressing the nonlinear threshold effect of ground-ice on reindeer population dynamics. The exponent is arbitrarily chosen to give a parabolic relation; improved fits to the data can be obtained by adjusting the exponent (in this case the best fit exponent for the regression is 2.6). While the data series is too short to explore the nature of such threshold patterns in detail, we can reach the same fundamental conclusions in this section with just a linear regression. In the latter case the regression coefficients are lower (e.g. Fig. 9) when using all of the data (i.e. Table 3a), but are essentially the same for the censored regressions.

## Conclusion

Previous studies on Svalbard reindeer dynamics have shown that a relatively large proportion of the variance in population growth rate fluctuations can be explained from the amount of winter precipitation (Aanes et al., 2000, 2003). In this paper we refine our understanding of the importance of winter climate by decomposing winter precipitation amounts into snow and ground-ice components in the study area, using a simple modeling approach, and show that simulated ground-ice thickness is by far the best single parameter to explain the variance in reindeer population growth rate.

The ideal on study arctic population would include long time-series of *in situ* data on snowdepth, quality of snow (e.g., ice layers in the snow) and ground-ice thickness; such measurements are rarely, if ever, available to field ecologists, at least not over longer time spans. The simple modeling approach outlined in this paper provides a viable alternative given that standard measurements of precipitation and temperature usually available from meteorological stations close to a given study area. Our results show that the simple model is adequate to explain snowpack effects when evaluating mechanisms underlying often-observed fluctuations in large herbivores, with special emphasis to arctic areas.

The simplicity of the model allows rapid exploration of adjustable parameters, which may be necessary when extrapolating meteorological measurements made at one site to an entire landscape or region. This points to another direction forward, which is to consider the spatial or elevational dependence of snowpack characteristics. For example, we have observed reindeer foraging at high altitudes in the

steep mountainous areas of Brøgger peninsula during winters with deep snow, or with ground-ice. It also remains to investigate what is available in these higher foraging grounds. The vegetation in the area is commonly mapped below the 200-m contour line (Brattbakk, 1986). If available forage above this height mainly consists of lichens it is plausible to believe that there are no large quantities, and the regrowth of lichens are extremely slow. Hence, such foraging refuges may be overgrazed rapidly if repeated blocking of food on the lowland plain happens.

Finally, another step forward in implementing the snowpack model is to drive the model with future climate scenarios. For example, a simple population dynamics relation of the type implied by the regressions summarized in Table 3 would then allow prediction of the future for Svalbard reindeer. As pointed out by Putkonen and Roe (2003), the frequency of climatic conditions which result in winter ground-ice may increase substantially in the future as climate shifts toward warmer and wetter winters, suggesting that more ground-icings are likely and that the future may be challenging for Svalbard reindeer.

## Acknowledgments

We are indebted to Nils Are Øritsland who conceived and implemented the introduced reindeer experiment at Brøgger peninsula. We would further like to thank Erling J. Solberg and Regine Hock for comments which substantially improved the organization and readability of the paper. We are grateful to the Norwegian Meteorological Institute for providing data. R. Aanes was partly funded by the Norwegian Research Council through the KlimaEffekt programme (project no. 155903/720).

## References Cited

- Aanes, R., Sæther, B.-E., and Øritsland, N. A., 2000: Fluctuations of an introduced population of Svalbard reindeer: the effects of density dependence and climatic variation. *Ecography*, 23: 437–443.
- Aanes, R., Sæther, B.-E., Smith, F. M., Cooper, E. J., Wookey, P. A., and Øritsland, N. A., 2002: The Arctic Oscillation predicts effects of climate change in two trophic levels in a high-arctic ecosystem. *Ecology Letters*, 5: 445–454.
- Aanes, R., Sæther, B.-E., Solberg, E. J., Aanes, S., Strand, O., and Øritsland, N. A., 2003: Synchrony in Svalbard reindeer population dynamics. *Canadian Journal of Zoology*, 81: 103–110.
- Adamczewski, J. Z., Gates, C. C., Soutar, B.-M., and Hudson, R. J., 1988: Limiting effects of snow on seasonal habitats use and diets of caribou (*Rangifer tarandus groenlandicus*) on Coat Island; North West Territories. *Canadian Journal of Zoology*, 66: 1986–1996.
- Alendal, E. and Byrkjedal, I., 1974: Population size and reproduction of the reindeer (*Rangifer tarandus platyrhynchus*) on Nordenskiöld Land, Svalbard. Norsk Polarinstitutt Årbok 1974, 139–152.
- Bartelt, P. and Lehning, M., 2002: A physical SNOWPACK model for the Swiss avalanche warning. Part I: numerical model. *Cold Regions Science Technology*, 35: 123–145.
- Boike, J., Roth, K., and Ippisch, O., 2003: Seasonal snow cover on frozen ground: Energy balance calculations of a permafrost site near Ny-Ålesund, Spitsbergen. *Journal of Geophysical Research*, 108(D2), doi: 10.1029/2001JD000939.
- Braithwaite, R. J., 1995: Positive degree-day factors for ablation on the Greenland ice-sheet studied by energy-balance modeling. *Journal of Glaciology*, 41: 153–160.
- Brattbakk, I. 1986: Flora and vegetation. In Øritsland, N. A. (ed.), *Svalbardreinen og dens livsgrunnlag*. Oslo: Universitetsforlaget, 15–34.
- Cooper, E. J. and Wookey, P. A., 2001: Field measurements of the growth rates of forage lichens and the implications of grazing by Svalbard reindeer. *Symbiosis*, 31: 173–186.
- Coulson, T., Catchpole, E. A., Albon, S. D., Morgan, B. J. T., Pemberton, J. M., Clutton-Brock, T. H., Crawley, M. J., and



- Grenfell, B. T., 2001: Age, sex, density, winter weather, and population crashes in Soay sheep. *Science*, 292: 1528–1531.
- Davis, J. C., 2002: *Statistics and Data Analysis in Geology*. 3rd ed. New York: J. Wiley. 638 pp.
- Fancy, S. G., and White, R. G., 1985: Energy expenditures of caribou while cratering in snow. *Journal of Wildlife Management*, 49: 987–993.
- Forchhammer, M. C., and Boertmann, D., 1993: The muskoxen *Ovibos moschatus* in north and north-east Greenland: population trends and the influence of abiotic parameters on population dynamics. *Ecography*, 16: 299–308.
- Førland, E. J., Hanssen-Bauer, I., and Nordli, P. Ø., 1997: Orographic precipitation at the glacier Austre Brøggerbreen, Svalbard. *DNMI-Report 2/97 KLIMA*. 45 pp.
- Førland, E. J. and Hanssen-Bauer, I., 2000: Increased precipitation in the Norwegian Arctic: True or false? *Climatic Change*, 46: 485–509.
- Gaillard, J. M., Festa-Bianchet, M., and Yoccoz, N. G., 1998: Population dynamics of large herbivores: variable recruitment with constant adult survival. *Trends in Ecology and Evolution*, 13: 58–63.
- Gaillard, J. M., Festa-Bianchet, M., Yoccoz, N. G., Loison, A., and Toigo, C., 2000. Temporal variation in fitness components and population dynamics of large herbivores. *Annual Review of Ecology and Systematics*, 31: 367–393.
- Grenfell, B. T., Wilson, K., Finkenstadt, B. F., Coulson, T. N., Murray, S., Albon, S. D., Pemberton, J. M., Clutton-Brock, T. H., and Crawley, M. J., 1998: Noise and determinism in synchronized sheep dynamics. *Nature*, 394: 674–677.
- Henriksen, S., Aanes, R., Sæther, B.-E., Ringsby, T. H., and Tufto, J., 2003: Does availability of resources influence grazing strategies in female Svalbard reindeer? *Rangifer*, 23: 25–37.
- Hock, R., 1999: A distributed temperature-index ice- and snowmelt model including potential direct solar radiation. *Journal of Glaciology*, 45: 101–111.
- Hock, R., 2003: Temperature index melt modelling in mountain regions. *Journal of Hydrology*, 282: 104–115.
- Jordan, R., 1991: A one-dimensional temperature model for a snow cover: Technical documentation for SNTherm.89. U. S. Army Cold Regions Research and Engineering Laboratory, Hanover, NH. *Special Report 91-16*.
- Larsen, T., 1976: Counts and population estimates of Svalbard reindeer (*Rangifer tarandus platyrhynchus*) in Nordaustlandet, Svalbard, 1974 and 1976. *Norsk Polarinstitutt Årbok 1976*, 243–248.
- Lefebvre F., Gallee H., Van Ypersele J. P., and Huybrechts P., 2002: Modelling of large-scale melt parameters with a regional climate model in south Greenland during the 1991 melt season. *Annals of Glaciology*, 35: 391–397.
- Lefauconnier, B., Hagen, J.-O., Ørbæk, J. B., Melvold, K., and Isaksson, E., 1999: Glacier balance trends in the Kongsfjord area, western Spitsbergen, Svalbard, in relation to the climate. *Polar Research*, 18: 307–313.
- Lindström, G., Johansson, B., Persson, M., Gardelin, M., and Bergström, S., 1997: Development and test of the distributed HBV-96 hydrological model. *Journal of Hydrology*, 201: 272–288.
- Lønø, O., 1959: Reinen på Svalbard. *Norsk Polarinstitutt Meddelelser*, 83: 1–31.
- Øritsland, N. A., 1998: Reindeer population size and trend on Edgeøya Svalbard. *Polar Research*, 17: 101–105.
- Øritsland, N. A., Ødegaard, H., Frøyland, E., and Brattbakk, I., 1980: Use of satellite data and the IBM-ERMAN system in mapping of reindeer grazing range on Svalbard. In Reimers, E., Gaare, E., and Skjenneberg, S. (eds.). *Proceedings 2nd International Reindeer/Caribou Symposium, Røros, Norway 1979*. Direktoratet for vilt og ferskvannsfisk, 174–177.
- Parker, G. R., Thomas, D. C., Broughton, E., and Gray, D. R., 1975: Crashes of muskox and Peary caribou populations in 1973–74 on the Parry Islands, Arctic Canada. *Canadian Wildlife Services, Progress Notes*, 56.
- Post, E. and Stenseth, N. C., 1999: Climate change, plant phenology, and northern ungulates. *Ecology*, 80: 1322–1339.
- Post, E. and Forchhammer, M. C., 2003: Synchronization of animal population dynamics by large-scale climate. *Nature*, 420: 168–171.
- Putkonen J., 1998: Soil thermal properties and heat transfer processes near Ny-Ålesund, northwestern Spitsbergen, Svalbard. *Polar Research*, 17: 165–179.
- Putkonen J. and Roe, G., 2003: Rain-on-snow events impact soil temperatures and affect ungulate survival. *Geophysical Research Letters*, 30(4) doi: 10.1029/2002GL016326.
- Rango, A. and Martinec, J., 1995: Revisiting the degree-day method for snowmelt computations, *Water Resource Bulletin*, 31: 657–669.
- Reimers, E., 1977: Population dynamics in two subpopulations of reindeer in Svalbard. *Arctic and Alpine Research*, 9: 369–381.
- Reimers, E., 1982: Winter mortality and population trends of reindeer on Svalbard, Norway. *Arctic and Alpine Research*, 14: 295–300.
- Reimers, E., 1983: Mortality in Svalbard reindeer. *Holarctic Ecology*, 6: 141–149.
- Roth, K. and Boike, J., 2001: Quantifying the thermal dynamics of a permafrost site near Ny-Ålesund Svalbard, *Water Resources Research*, 37: 2901–2914.
- Solberg, E. J., Strand, O., Jordhøy, P., Aanes, R., Loison, A., Sæther, B.-E., and Linnell, J. D. C., 2001: Effects of density-dependence and climate on the dynamics of a Svalbard reindeer population, *Ecography*, 24: 441–451.
- Sæther, B.-E., 1997: Environmental stochasticity and population dynamics of large herbivores: a search for mechanisms. *Trends in Ecology and Evolution*, 12: 143–149.
- Tyler, N. J. C., 1987: Natural limitation of the abundance of the high arctic Svalbard reindeer. PhD thesis. University of Cambridge, Cambridge.

*Mss submitted February 2004*